Ion Distribution at Steel/Concrete Interface in Steel Reinforced CSA Concrete by Newly Updated Image Analysis Technique

IOP Conf. Series: Materials Science and Engineering **585** (2019) 012079 doi:10.1088/1757-899X/585/1/012079

Ion Distribution at Steel/Concrete Interface in Steel Reinforced CSA Concrete by Newly Updated Image Analysis Technique

Meimei Song[1, *], Chuanlin Wang[2]

[1]Department of Mechanical Engineering, Xi'an Shiyou University, Xi'an 710065, China
[2]College of Engineering, Shantou University, Shantou, 515063, China
[*]Email: mmsong@xsyu.edu.cn

Abstract. Calcium sulfoaluminate (CSA) cement is potential low-carbon cement; therefore investigation on ion exchange property at the steel/concrete interface is of great importance to understand the corrosion resistance and long-term durability properties of steel reinforced CSA concrete. Moreover, there is still a lack of standard procedure for quantitative imaging analysis in the study of cementitious materials so far. In this study, we developed an updated imaging analysis technique to investigate the atomic information in steel reinforced CSA concrete by using quantified elemental mappings. Microstructure of steel reinforced CSA concretes were characterized by SEM/EDX. The results indicated that there was less active ion distribution at the steel/concrete interface in CSA concrete than that for OPC concrete. Al/Ca ratio decreased over the interfacial zone gradually with ageing period of up to 1.5 years, but Al still dominated in the CSA concrete compared to the OPC concrete.

1. Introduction

For conventional steel reinforced Portland concrete, reinforcement corrosion is one of the main causes of deterioration of reinforced concrete structures, arising as a worldwide concern in the construction industry. CSA cement is a low-carbon binder with high early strength and improved durability. Recent research on CSA cement mainly focuses on the hydration mechanism [1-5] as well as cement clinker modification with the addition of industry wastes [6-9]. The popularity of CSA cement, used as a potential low-carbon binder, encourages the studies on steel reinforced CSA concrete systems, particularly focusing on the corrosion resistance capability of the rebar embedded in this newly modified CSA-based material. Up to date there is still a lack of microstructure studies at the steel/concrete interface in steel reinforced CSA cement systems in literature, which is one of the intrinsic factors in deciding composite durability properties. Whether or not preferential accumulation of different ions is occurring at the interface still remains unknown. And it is necessary to further investigate the distribution of different atomic ratios such as Ca/Si, Al/Ca, S/Ca as a function of certain distance away from steel. This useful information facilitates a straightforward interpretation of the chemicals present at the interface and can also reflect the ion distribution properties at this region over curing, which is eventually responsible for the corrosion resistance of reinforcement embedded in CSA concrete systems.

Investigation of the microstructure in concretes by backscattered electron microscopy has become a common technique nowadays; it is a powerful tool for the study of cementitious materials. This technique is able to provide useful information on the porosity [10], pore structures [11] and phase distribution within the cement system. These beneficial advantages lead to extensive studies on

developing useful image analysis programs to add quantitative information to the analysis at the interface [12-18]. It is expected to achieve the following two tasks.

- Phase segmentation by morphological features and/or arithmetic process
- Quantitative measurements on the area fraction of each segmented phase

Although the achieved quantification at the steel/concrete interface can provide useful information on both microstructural and compositional features of this region, there are no standard procedures established for the phase segmentation. Different methodologies applied in different studies can cause user-bias. Moreover, the existing image analysis techniques are not productive and they are only unique for one specific cementitious material, e.g. threshold values for phase segmentation need to be adjusted for different concrete mixing designs. Therefore an updated image analysis technique with a wider range of applications (i.e. varying mixing designs for both hydrated Portland cement and non-Portland cement systems) becomes very imperative to reflect increases in image processing power, consequently giving much more accurate results on quantitative analysis. In previous studies on quantitative analysis, elemental mappings were used to assist phase segmentation as it could provide straightforward spatial distribution of selected elements [9]. In the present study, elemental mappings are obtained with much longer acquisition time (dwell time of 1000μs) and are quantified in pixel.

This paper describes the process of a newly updated imaging analysis technique in order to standardize the quantitative analysis procedure, which is expected to be applicable for all cementitious materials with less user bias. Meanwhile, atomic data over the steel/concrete interface is also present in order to understand ion distribution properties, microstructure evolution and therefore durability performance in the steel reinforced CSA concretes.

2. Experimental Investigation

The commercial CSA cement used in the study of steel reinforced concrete system was provided by Hanson Heidelberg Cement Group and chemical composition of CSA cement and traditional Portland cement was present in Table.1.

Steel reinforced concrete cubes (100mm×100mm×100mm) were prepared with four round bright steel bars with a diameter of 10mm, they were inserted vertically into the concrete during casting. Before casting, those bars were cleaned with acetone in order to remove loose rust and grease left on the surfaces. The mix design for the CSA concrete and conventional Portland concrete was present in Table.2. Thin section petrographic (TSP) specimens for steel reinforced CSA and OPC concrete, with a longitudinally sectioned steel bar located in the middle of glass slide, were produced (thickness ~30μm) at ages of 28d and 1.5y. Slides were covered by a cover slip immediately after finishing and kept in a low-CO2 desiccator. For later SEM analysis, the cover slip was removed by gentle sliding.

Table 1. Chemical composition of cement clinkers of CSA cement and Portland cement

Oxide	CaO	SiO_2	Al_2O_3	SO_3	MgO	FeO_2	K_2O	SrO	Mn_3O_4	TiO_2	LOI
	42.33	9.0	33.82	8.83	2.29	1.35	0.22	0.07	0.03	1.61	0.45

Table. 2 Mix design of CSA concrete

CSA cement (kg/m^3)	Water (kg/m^3)	Fine aggregate (kg/m^3)	Coarse aggregate (kg/m^3)	w/c (%)
309	136	740	1100	0.44

SEM was undertaken by JEOL JSM-5800LV, which was also equipped with energy dispersive X-ray (EDX) detector. Backscattered electron mode was chosen to characterize the steel/matrix interfacial zone. Elemental mappings were obtained with long acquisition time (dwell time of 1000μs). Fifteen BSE images (size of 512×384 pixel) and the corresponding elemental mappings were collected for both samples at each specific age with Inca software by Smartmap function (as shown in Fig.1).

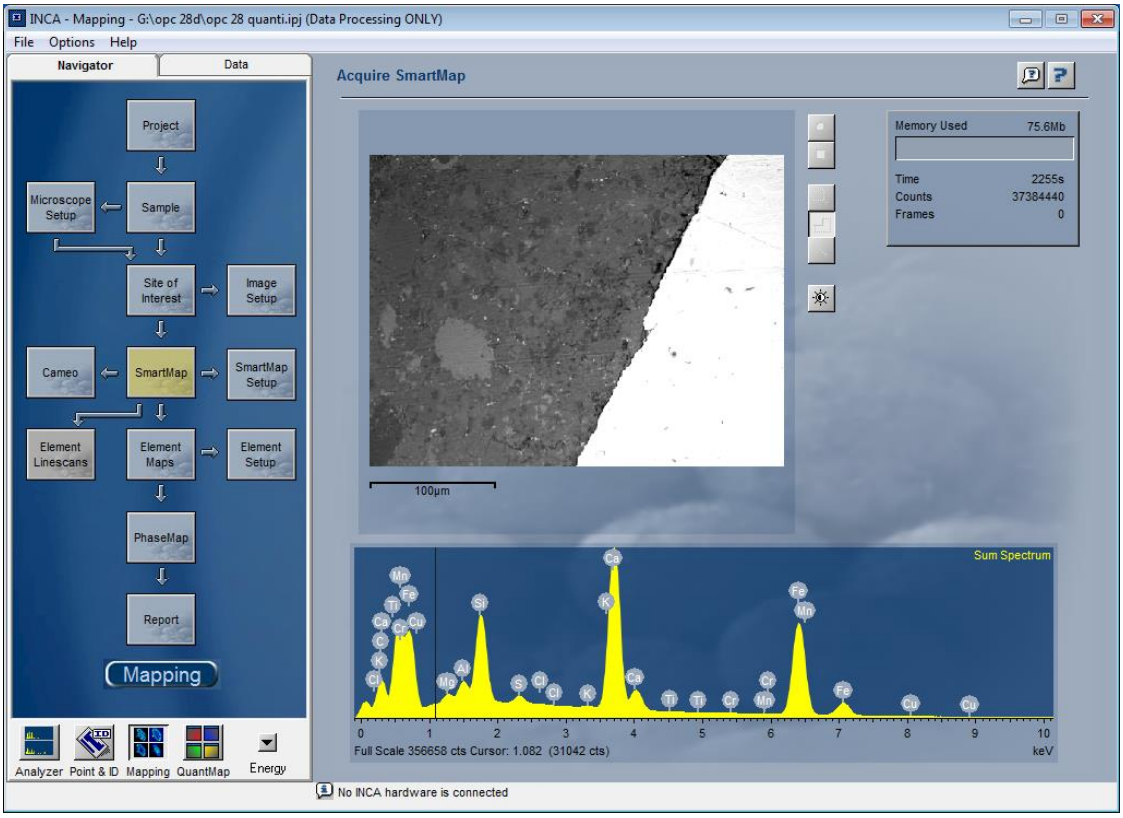

Figure 1. "Smartmap" function to acquire elemental mappings in Inca software

The atomic information obtained in each mapping was then read pixel by pixel by the QuantMap function in Inca, finishing with an Excel (Mocrosoft® Office Excel 2007) spreadsheet containing 384 rows and 512 columns (same size as the obtained backscattered electron images, as shown in Fig.2 and Fig.3). Each cell was representative of the pixel at exactly the same location in corresponding element mapping. Excel (Mocrosoft® Office Excel 2007) sheet for iron mapping was used to extract the atomic data at the steel/concrete interface. A macro written in MATLAB® (r2013b; Math Works Inc.) was established to find the edges of reinforcement first, as indicated by a huge difference of atomic number at steel edges. Followed by this, the edge layer was then expanded by extracting another 25 pixels data vertically, accumulating for ~30µm in width which was supposed to contain the interfacial information. If the cell location in the steel mapping was recorded in a MATLAB® (r2013b; MathWorks Inc.) macro, corresponding data for other elements (i.e. Ca, Si, S, Al) could thus be extracted in Excel (Mocrosoft® Office Excel 2007) sheet. Consequently, atomic ratios at interfacial zone can therefore be obtained by arithmetic calculation. This quantitative analysis methodology is highly reproducible and reliable as no user-bias is introduced.

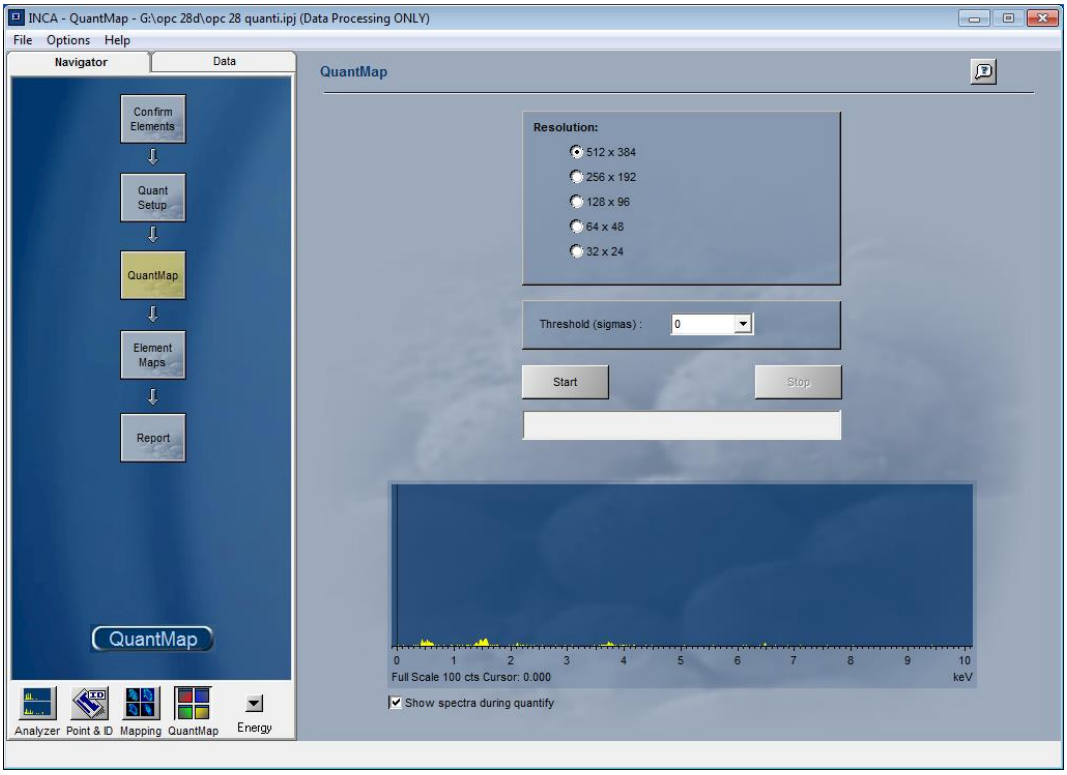

Figure 2. Extraction of atomic information in elemental mappings by Quantmap function in Inca software

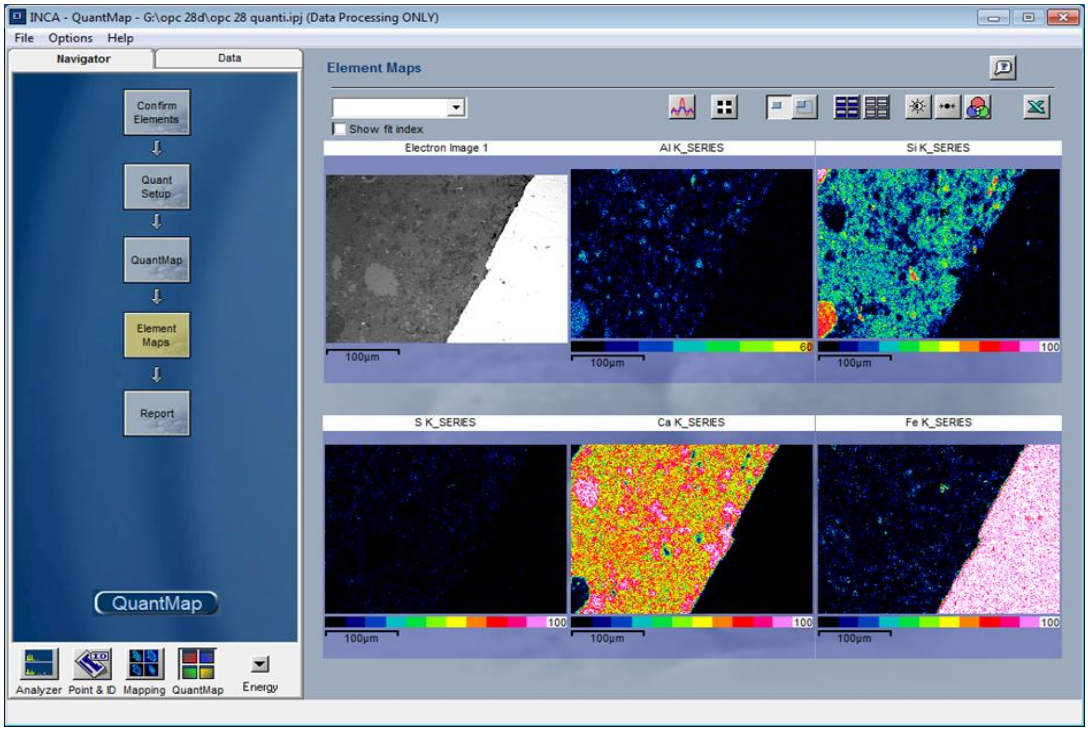

Figure 3. Examples of to export Excel spreadsheet for ion information in Inca software

3. Results and Discussion

3.1 Microstructure of Interface at Steel Reinforced CSA Concrete

Microstructure of interface at steel reinforced CSA concrete is present in Fig.4. Phases of interests such as unhydrated cement, hydration products (ettringite, AH_3, CAH_{10} etc.) and porosity can be differentiated according to individual grey scale, which greatly depends on electron density of the materials. Steel bar displays as the lightest in Fig.4.a, surrounded by a continuous rust layer with a thickness of about 22 μm. Within the concrete matrix, unhydrated cement clinker can be easily identified due to its lightest grey scale (excluding steel bars). An enlarged BSE image of the matrix shows that large voids tended to be filled with ettringite, with lengths of about 10 μm and forming interlocking network.

At the interfacial zone, CSA cement paste has an intimate contact with the reinforcement and few air voids are observed in the vicinity of steel. The corresponding porosity data is shown in Fig.4.b, as a function of distance from steel surface. It is clear that the interfacial zone within the first 25μm is much less porous than that in the bulk matrix. Therefore pore-solution mediated current flow between anode and cathode should be relatively restricted at the interface, which would result in reduced possibility that electrochemical reactions would happen. According to the element mapping (Fig.4.d), there is a large amount of Al clustered at the interface intensively. A very thin sulfur layer is accumulated along part of rebar, which is probably AFt or AFm phases given the association with the Al (and to a less extent Ca) mapping. EDX analysis for representative Point '1' at the interface demonstrates a high Al/Ca ratio of 2.0 (Fig.4.c), compared to Al/Ca ratio of 0.33 for pure ettringite phase, 0.5 for AFm and 2.0 for pure CAH_{10} phase.

The current SEM results appear to confirm a less pronounced 'wall effect' of steel reinforcement in reinforced CSA concrete, as there is less porosity at the interface than that in the matrix. The embedded steel surface is surrounded by Al-enriched hydrating phases, which are presumably to be finely intermixed AH_3 (according to the intrinsic hydration of CSA cement) and other Ca-included hydration products (CAH_{10}, monosulfate etc., according to the Ca signal detected in the EDX analysis of Point '1'). These Al-enriched phases are postulated to protect the steel from corrosion by providing both buffering effect (due to high alkalinity of AH_3 [19]) as well as reduced porosity at the steel/concrete interface.

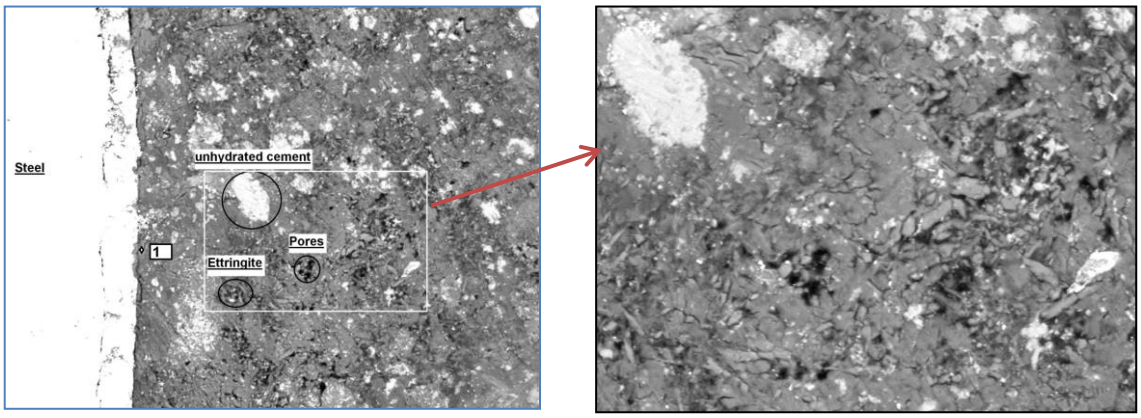

(a) BSE image of steel reinforced CSA concrete at a magnification of x400 (width of field 332 μm)

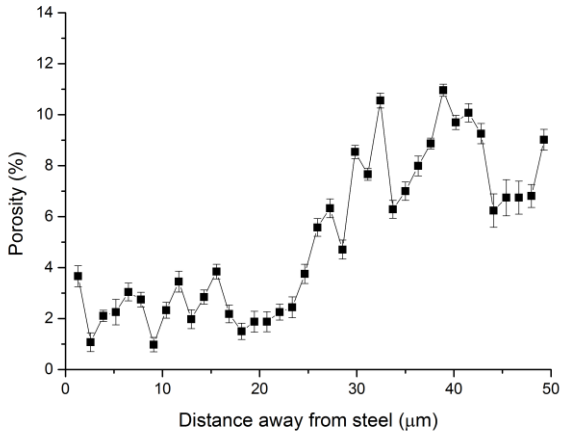

(b) Porosity vs. distance away from steel surface

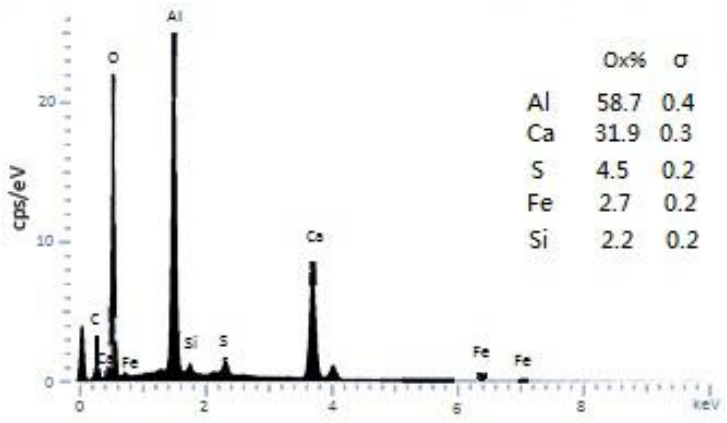

(c) Spot analysis on Point '1'

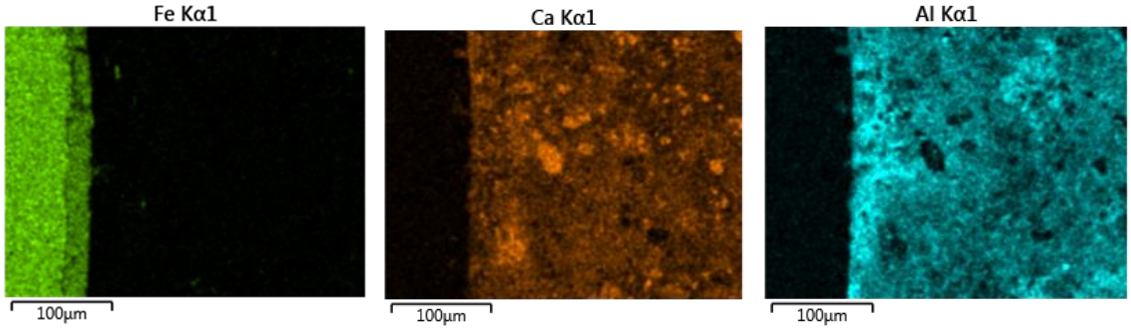

(d) Element mapping of Fe, Ca, Si, O, Al and S in Fig.3.a, at a magnification of ×400. Much more Al is precipitated at interfacial zone than the bulk matrices

Figure 4. Backscattered electron image of steel reinforced CSA concrete aged for 28 days

3.2 Image Analysis

Image analysis results of steel reinforced CSA for both 28d and 1.5y are present in Fig.5, focusing on the distribution of atomic ratios at the interfacial zone as a function of distance away from steel surface. Fifteen BSE images were randomly selected for each sample at each specific curing age, together with the corresponding elemental mappings. Error bars of standard deviations are added in each set of data to demonstrate statistical significance.

In the 28d-aged sample, Ca to Si (Fig.5.a) ratio starts at ~2.0 near rebar surface; it then exhibits slight increase along interface and reaches 2.5 at 30μm away from steel. In the 1.5y-aged sample, Ca/Si ratio shows insignificant fluctuation and stays at ~2.5 over the interface. In general, extremely high Al/Ca ratio of over 1.0 (in Fig.5.b) in the CSA sample can be observed, albeit it shows decreasing Al/Ca ratio along the interfacial area with the progress of hydration at both curing ages. For example, the Al/Ca ratio reduces from 2.5 to 1.5 in the 28d sample and a lower range from 1.5 to 1.0 is clear in the 1.5y sample. The overall Al/Ca reduction in the 1.5y-sample can be explained by the continuous consumption of AH_3 with belite, leaving the generation of stratlingite in hydrated CSA cement. The corresponding error bars are within an acceptable range of 0.4. The dominance of Al refers to the formation of amorphous AH_3, which is one of the main hydration products of CSA cement. High alkaline of AH3 helps to maintain alkaline chemical environment near the embedded rebar. Almost no obvious changes in S/Ca ratio with age (in Fig.5.c) can be observed.

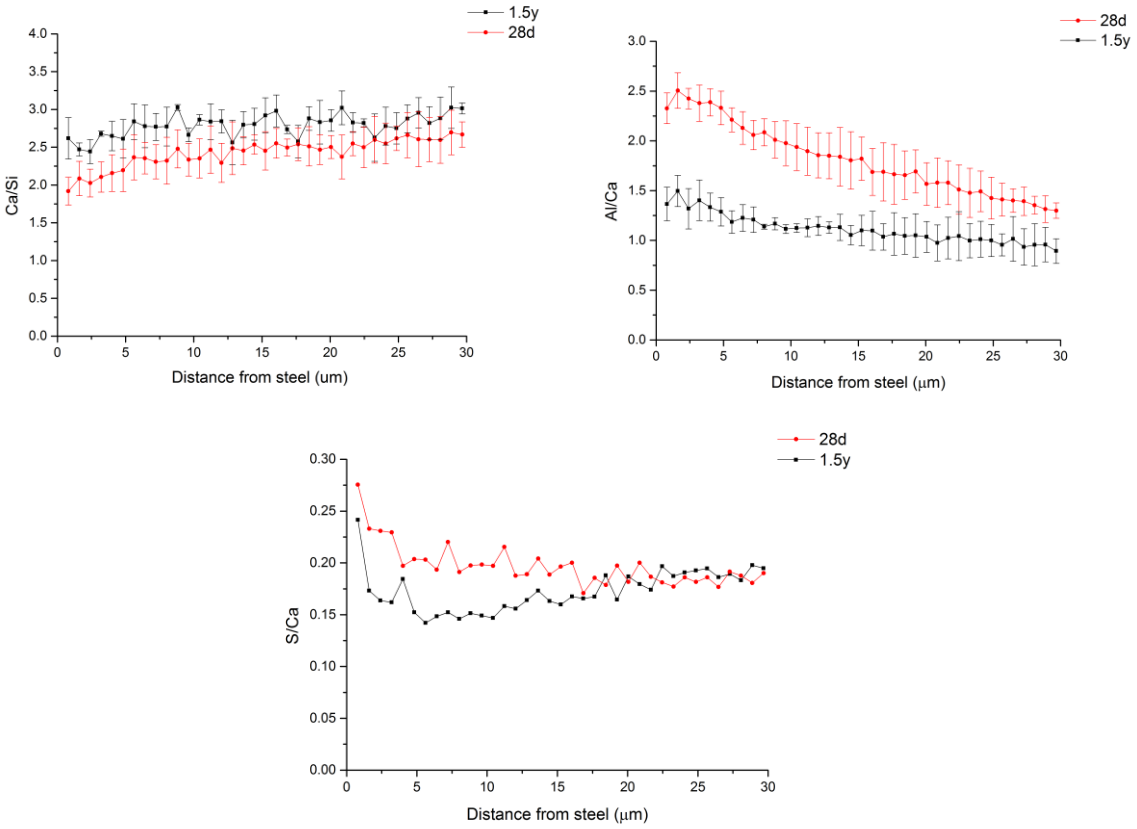

Figure 5. Image analysis on atomic ratios at the steel/concrete interface in reinforced CSA concrete

4. Conclusions

Ion distribution and mitigation are prone to be limited at the steel/concrete interface in the hydrated CSA cement, thus can provide a relatively less-active chemical environment for the embedded steel reinforcements. Al to Ca ratio decreases steadily over the interfacial zone in steel reinforced CSA concrete at both investigated ages, but it still dominates greatly than that in the OPC concrete. The dominance of Al at interfacial region refers to amorphous AH_3, which helps to maintain high alkaline near rebar. Newly updated imaging analysis technique is capable to provide quantitative data on the atomic information within any selected area in backscattered images, this opens the age of more accurate and user bias-free quantification analysis for cementitious materials.

5. Acknowledgment
This work is funded by National Natural Science Foundation of China (51674199) and Scientific Research Project of Shaanxi Education Department (18JK0618).

6. References

[1] Trauchessec R, Mechling J M, Lecomte A, et al. 2015. Hydration of ordinary Portland cement and calcium sulfoaluminate cement blends. Cement & Concrete Composites, 56, pp. 106-114.
[2] Liao Y, Wei X, Li G. 2011. Early hydration of calcium sulfoaluminate cement through electrical resistivity measurement and microstructure investigations. Construction & Building Materials, 25(4), pp. 1572-1579.
[3] Telesca A, Marroccoli M, Pace M L, et al. 2014. A hydration study of various calcium sulfoaluminate cements [J]. Cement & Concrete Composites, 53(10), pp. 224–232.
[4] Song F, Yu Z, Yang F, et al. 2015. Microstructure of amorphous aluminum hydroxide in belite-calcium sulfoaluminate cement. Cement & Concrete Research, 71, pp. 1-6.
[5] Tang S W, Zhu H G, Li Z J, et al. 2014. Hydration stage identification and phase transformation of calcium sulfoaluminate cement at early age. Construction & Building Materials, 75, pp. 11-18.
[6] Garc á M. 2013. Hydration studies of calcium sulfoaluminate cements blended with fly ash. Cement & Concrete Research, 54, pp. 12-20.
[7] Chen I A, Juenger M C G. 2012. Incorporation of coal combustion residuals into calcium sulfoaluminate-belite cement clinkers. Cement & Concrete Composites, 34(8), pp. 893-902.
[8] Berger S, Coumes C C D, Champenois J B, et al. 2011. Stabilization of ZnCl 2 -containing wastes using calcium sulfoaluminate cement: Leaching behaviour of the solidified waste form, mechanisms of zinc retention. Journal of Hazardous Materials, 194(5), pp. 268-276.
[9] Chaunsali P, Mondal P. 2014. Influence of Mineral Admixtures on Early-Age Behavior of Calcium Sulfoaluminate Cement. Aci Materials Journal, 111, pp. 1-6.
[10] WONG, H. S., M. K. HEAD and N. R. BUENFELD. 2006. Pore segmentation of cement-based materials from backscattered electron images. Cement and Concrete Research, 36(6), pp. 1083-1090.
[11] WERNER, A. M. and D. A. LANGE. 1999. Quantitative image analysis of masonry mortar microstructure. Journal of Computing in Civil Engineering, 13(2), pp. 110-115.
[12] HORNE, A. T., I. G. RICHARDSON and R. M. D. BRYDSON. 2007. Quantitative analysis of the microstructure of interfaces in steel reinforced concrete. Cement and Concrete Research, 37(12), pp. 1613-1623.
[13] DIAMOND, S. 2001. Considerations in image analysis as applied to investigations of the ITZ in concrete. Cement & Concrete Composites, 23(2-3), pp. 171-178.
[14] DIAMOND, S. and J. D. HUANG. 2001. The ITZ in concrete - a different view based on image analysis and SEM observations. Cement & Concrete Composites, 23(2-3), pp. 179-188.
[15] GLASS, G. K., R. YANG, T. DICKHAUS and N. R. BUENFELD. 2001. Backscattered electron imaging of the steel-concrete interface. Corrosion Science, 43(4), pp. 605-610.
[16] YANG, R. and N. R. BUENFELD. 2001. Binary segmentation of aggregate in SEM image analysis of concrete. Cement and Concrete Research, 31(3), pp. 437-441.
[17] DESCHNER, F., B. MUENCH, F. WINNEFELD and B. LOTHENBACH. 2013. Quantification of fly ash in hydrated, blended Portland cement pastes by backscattered electron imaging. Journal of Microscopy, 251(2), pp. 188-204.
[18] STUTZMAN, P. 2004. Scanning electron microscopy imaging of hydraulic cement microstructure. Cement & Concrete Composites, 26(8), pp. 957-966.
[19] Quillin, K., Performance of belite-sulfoaluminate cements. Cement and Concrete Research, 2001. 31(9): p. 1341-1349.